06.5;15.1

Studying $LiFePO_4$ powder samples via X−ray diffraction techniques using artificial neural networks

© M.E. Boiko, M.D. Sharko, A.M. Boiko, A.V. Bobyl, V.I. Nikolaev

Ioffe Institute, St. Petersburg, Russia
E-mail: mischar@mail.ru, boikomix@gmail.com

Received April 5, 2022
Revised May 17, 2022
Accepted May 30, 2022

A set of $LiFePO_4$ samples has been studied by small−angle X−ray scattering (SAXS). Using the technique of artificial neural networks, the shape of SAXS curves has been reconstructed taking into account the hardware function. Estimates of homogeneitiesśizes and shapes in the studied $LiFePO_4$ samples have been obtained.

Keywords: Small−angle X−ray scattering, artificial neural network, lithium−ion rechargeable batteries, incorrect tasks regularization.

DOI: 10.21883/TPL.2022.07.54040.19214

One of the up−to−date research fields of a great topicality and practical importance is studying lithium−iron battery materials, including lithium−iron phosphate ($LiFePO_4$) used as cathodic material; $LiFePO_4$ is a *Pnma* (№ 62) orthorhombic crystal [1] with lattice parameters $a = 10.328$ Å, $b = 6.007$ Å, $c = 4.694$ Å.

In this work, dimensions and geometric features of homogeneous $LiFePO_4$ phases were investigated by small−angle X−ray scattering (SAXS) using a set of five samples (hereinafter, samples№ 1−5) obtained by chemical methods [2].

The SAXS technique is known [3] to ensure estimation of a homogeneity size (Guinier gyration radius) and curveś intensity attenuation coefficient (Porod index) dependent on the particle geometry. The Porod index for low−size particles roughly matches with their dimension; in 3D powders, it is about 4 [3,4].

The set of $LiFePO_4$ powders to be studied consists of four commercial samples and one test sample [2,5] synthesized by the liquid−phase method accompanied by thermal treatment [2]. As in [2,5], commercial samples are designated as № 1−3, 5, while the test one is designated as№ 4. Powder samples $LiFePO_4$ were shaped as pellets no more than 1 mm in thickness. Earlier the same set of samples was studied by transmission electron microscopy (TEM) and X−ray diffraction (XD), and data obtained were analyzed.

Fig. 1, *a* presents a TEM photo obtained at the Ioffe Institute by using electron microscope JEM-2100F Jeol (the figure was furnished by V.N. Nevedomsky). Fig. 1, *b* demonstrates a histogram of the particle projection areas (in nm^2) visible in Fig. 1, *a*. The histogram shows that the characteristic size of homogeneous particles of the $LiFePO_4$ sample № 1 is 80−160 nm; the size of the major part of particle projections visible in the photo is about 150 nm. However, it turns out that the sample grain size dispersion is very high, and sizes of particles observed in the TEM photo may differ by several orders of magnitude.

XD data for all the studied samples were obtained at X−ray diffractometer Bruker Discover D8 (Saint Petersburg State University (SPSU)) [6] in the transmission mode with doublet $CoK_{\alpha 1,2}$ radiation. The obtained curves were processed based on the Williamson−Hall approach [7]. Analysis performed for a set of reflexes in the [100], [101], [210], [011] crystallographic directions in the $LiFePO_4$ matrix provided the following size estimates: 7−10 nm (for sample № 1), 8−23 nm (№ 2), 5−12 nm (№ 3), 10−30 nm (№ 4), 5−7 nm (№ 5). Since the analysis did not considered other broadening factors (e.g. the hardware function or thermal fluctuations enhancing the signal background components), the given values are the lower estimates of the real sizes of the $LiFePO_4$ grains.

SAXS data for the studied samples were obtained at X−ray diffractometer Bruker Discover D8 (SPSU) in the transmission mode with $CuK_{\alpha 1}$ radiation. To account for the instrument error, a scattering curve was measured along with the SAXS curves in the absence of the sample (direct beam signal) under the same conditions and with $CuK_{\alpha 1}$ radiation. The sample № 1 SAXS curve and direct beam curve are presented in Fig. 2.

The SAXS curves are susceptible to distortions caused by peculiar features of both the studied material and analyzing beam, i.e. they depend on the hardware function. Due to this, calculations obtained in processing the SAXS curves may appear to be significantly corrupted (for instance, the Guinier radius may be strongly underestimated because of the beam broadening). To reliably determine shapes and sizes of scattering objects, it may become necessary to reconstruct such a SAXS curve shape that the beam spatial form and energy spectrum could be described by the delta−function. This paper proposes to reconstruct the SAXS curve by the artificial neuron network (ANN) method [8,9].

The SAXS curve may be regarded as a convolution of the direct beam scattering function with respect to the wave

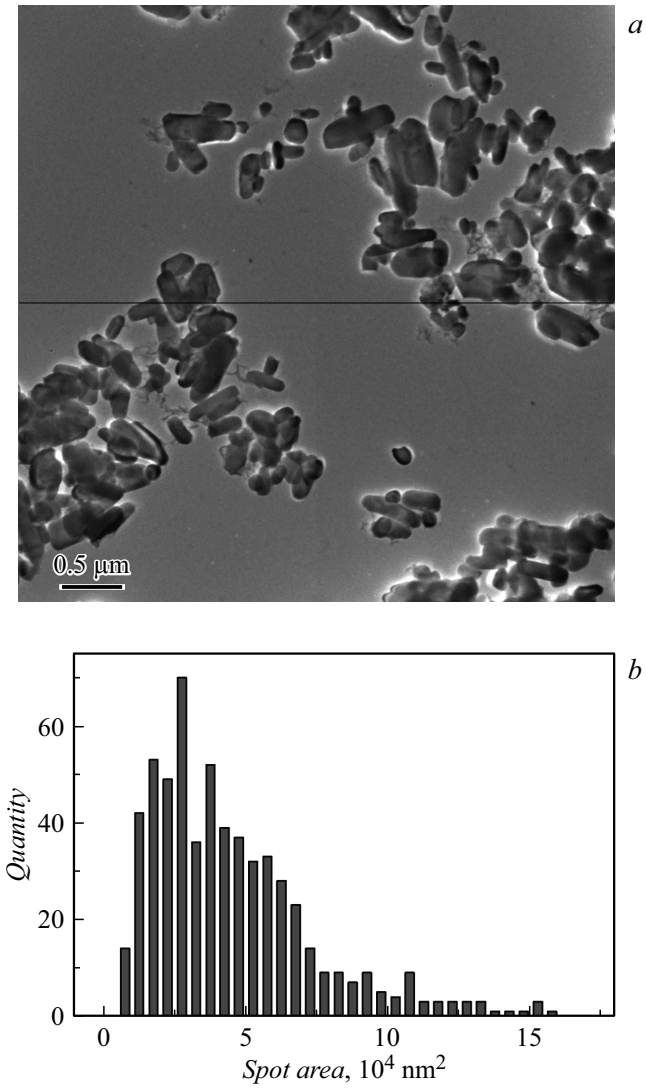

Figure 1. *a* — TEM data for the $LiFePO_4$ sample № 1 (the figure was furnished by V.N. Nevedomsky, Ioffe Institute); *b* — a histogram of particle sizes of the $LiFePO_4$ sample № 1.

vector with a hypothetical SAXS curve which could be obtained for an ideal beam (non–divergent and absolutely monochromatic). The convolution is formally reversible via Fourier transforms of the input and output functions; however, such a solution is unstable because noisy signals can create zeroes in the Fourier–transform image thus causing the „division-by-zero“error [10]. This difficulty may be overcome through analytical regularization providing stable solutions for high–power signals [10]. When the noise is relatively high, regularization suppresses the desired signal jointly with the noise. Fig. 3, *a* presents a curve obtained by using the Tikhonov regularization [10] of the deconvolution of the sample SAXS curve and direct beam scattering function. The curve contains a great number of singularities.

The direct reconstruction method consists in searching for such a model scattering curve that could minimize the deviation between the measured curve and curve obtained by convolution of the primary beam with the desired model curve. This method is in essence equivalent to the procedure for training a single–layer 320– point ANN [8]; in this case, the transmission curve calculation may be reduced to the problem of training a single–layer ANN with a linear activation function, where a set of initial data consists of a range of the primary beam values and one output signal value corresponding to this range.

To initiate the ANN training, it is necessary to choose a specific form of a normalizing functional characterizing the discrepancy of results, and also the general optimization method. Since initial data are characterized by a significant dispersion (most of values are lower than the maximum by a few orders of magnitude), the mean–square error did not provide a satisfactory estimation of the model; for this purpose, the relative error modulus was used. Nevertheless, in this case application of the gradient descent method and its analogs resulted in that the more the transmitted signal function is delta–like, the oftener are singularities in the desired function. The sample № 1 transmission function appeared to be sufficiently wide to make at least one of the involved ANN training methods ensure the absence of singularities.

In addition to the optimizer based on the gradient–descent method, the coordinate–descent method was applied, which, contrary to the first one, gave rise not to singularities but to oscillations near the minimum error. This approach allowed obtaining several hundreds of sets of weights with equal errors; further those values were averaged (taking into account the problem linearity). The total error of the averaged model did not exceed an error of each calculation model obtained by the coordinate–descent method; along with this, the processed diffraction curve was free of singularities.

Fig. 3, *b* demonstrates the results of reconstructing the sample № 1 SAXS curve by three different ANN–based techniques. Curve *1* was obtained using the gradient descent and mean–square error methods; this curve exhibits

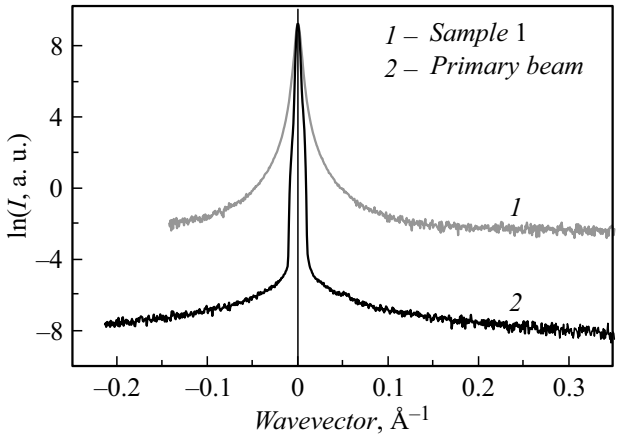

Figure 2. SAXS curves for the $LiFePO_4$ sample № 1 and direct beam.

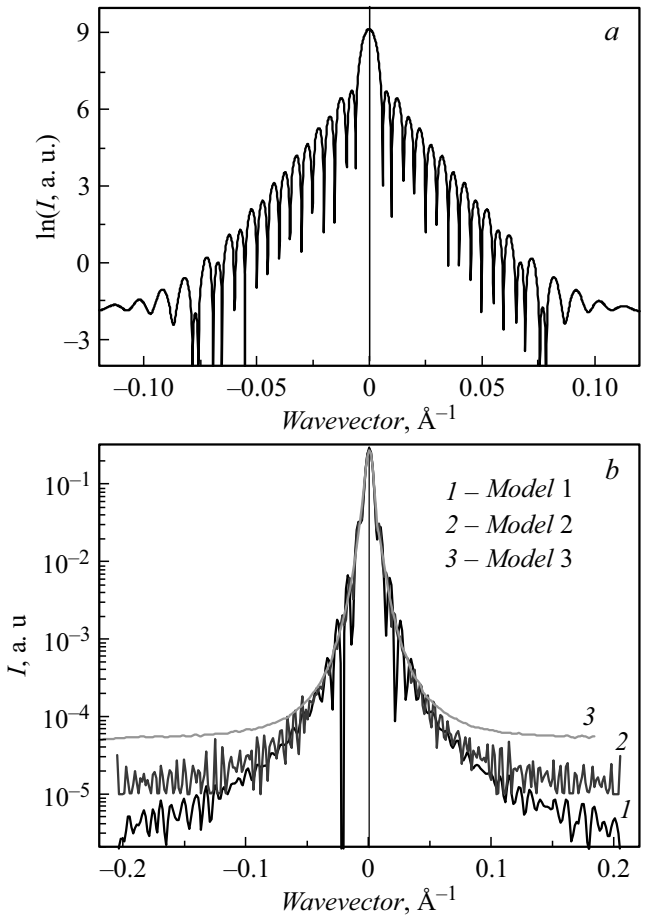

Figure 3. *a* — SAXS curve obtained by regularizing the inverse problem for sample № 1 after extracting from it the signal of the direct beam intensity by deconvolution with using the regularization method as per [10]; *b* — three models for reconstructing the shape of the sample № 1 SAXS curve based on the ANN technique: *1* — with gradient descent and mean–square error, *2* — with the Hadamard optimizer and relative error modulus, *3* — with coordinate descent, relative error modulus and averaging over 50 calculation variants.

singularities already in the vicinity of the zero peak, while in the Porod region the reconstructed curve gets destroyed becoming visually similar to noisy signals. Curve *2* was calculated based on the Hadamard optimizer and relative error modulus. In this case, the singularities shift away from the Guinier region towards the Porod regions where, however, the reconstructed curve gets destroyed similarly to curve *1*. Lastly, curve *3* is a result of calculation via the methods of coordinate descent, relative error modulus, and averaging over 50 variants of the calculation procedure. In this case, the reconstructed SAXS curve becomes smoothed and may be analyzed via both models, the Guinier and Porod ones. As Fig. 3, *b* shows, all the three calculation procedures coincide because in this region the problem is sufficiently well posed and singularities arise with decreasing weights (transmission coefficients).

Thus, two ways of solving the task of the SAXS curve shape reconstruction are proposed: by using the procedure of deconvolution regularization and by using the ANN mathematics.

In analyzing the SAXS curves reconstructed with the aid of regularized deconvolution, diameters of homogeneities (double Guinier radii) were obtained for all the samples (samples № 1–5) and appeared to range from 85 to 90 nm. Analysis of the Fig. 3, *a* singularities with the inverse regularization showed that they are caused by a too large scanning step and experimental noise, and their dips coincide with local derivative jumps on the noise peaks.

In its turn, the SAXS curve reconstructed by the ANN method with coordinate descent, relative error modulus and averaging over 50 variants of calculation (curve *3* in Fig. 3, *b*), i. e. the reconstructed curve free of singularities, provided after processing the following results. The double gyration radius proved to be about 55 nm, i. e. lower than in the case of using the regularized deconvolution. The Porod index on both sides of the direct beam peak was about 3. There exists a theoretical study [11,12] suggesting that Porod index 3 is associated with logarithmic fractals. The latter are structures where homogeneous fragments strongly (by orders of magnitude) differ in sizes; large grains are directly adjoined by smaller and more multiple homogeneities which in their turn may be surrounded by even smaller and more multiple neighbors.

The concept of dimensional hierarchy eliminates the contradiction between TEM photos exhibiting the predominance in the sample of particles more than 100 nm in size, SAXS data providing averaged sizes below 100 nm, and XD results demonstrating the phase dimensions of about 10 nm. TEM photos demonstrate projections of grain agglomerates which can overlap each other. The SAXS data are generated by regions homogeneous with respect to electron density, i. e. they are influenced by the agglomerate size (gyration radius) averaged in different directions. Lastly, XD provides the sizes of individual crystallites contained in agglomerates.

Thus, the paper shows that the ANN technique can ensure reconstruction of the SAXS curve shape free of singularities. Application of the ANN technique resulted in refining the basic characteristics of SAXS curves (attenuation coefficient, particle gyration radius) measured for the $LiFePO_4$ sample № 1. The developed approach is universal and applicable for investigating a wide range of solid–state materials.

Acknowledgements

The authors are grateful to V.N. Nevedomsky (Ioffe Institute) and I.A. Kasatkin (SPSU) for fruitful collaboration.

Conflict of interests

The authors declare that they have no conflict of interests.

References

[1] G. Liang, K. Park, J. Li, R.E. Benson, D. Vaknin, J.T. Markert, M.C. Croft, Phys. Rev. B, **77** (6), 064414 (2008). DOI: 10.1103/PhysRevB.77.064414
[2] A. Churikov, A. Gribov, A. Bobyl, A. Kamzin, E. Terukov, Ionics, **20** (1), 1 (2014). DOI: 10.1007/s11581-013-0948-4
[3] *Small-angle X-ray scattering*, ed by O. Glatter, O. Kratky (Academic Press, London, 1982).
[4] M.E. Boiko, M.D. Sharkov, A.M. Boiko, S.G. Konnikov, A.V.Bobyl', N.S. Budkina, Tech. Phys., **60** (11), 1575 (2015). DOI: 10.1134/S1063784215110067.
[5] E. Ershenko, A. Bobyl, M. Boiko, Y. Zubavichus, V. Runov, M. Trenikhin, M. Sharkov, Ionics, **23** (9), 2293 (2017). DOI: 10.1007/s11581-017-2068-z
[6] *Bruker D8 Series: User Manual, Version 6* (Bruker Corporation, Karlsruhe, 2018).
[7] G.K. Williamson, W.H. Hall, Acta Met., **1** (1), 22 (1953). DOI: 10.1016/0001-6160(53)90006-6
[8] S.S. Haykin, *Neural networks and learning machines* (Pearson Education, N.Y., 2009).
[9] Y.H. Hu, J.N. Hwang, *Handbook of neural network signal processing* (CRC Press, Boca Raton, 2002).
[10] A.N. Tikhonov, V.Ya. Arsenin, *Metody resheniya nekorrektnykh zadach* (Nauka, M., 1979). (in Russian)
[11] E.G. Iashina, E.V. Velichko, M.V. Filatov, W.G. Bouwman, C.P. Duif, A. Brulet, S.V. Grigoriev, Phys. Rev. E., **96** (1), 012411 (2017). DOI: 10.1103/PhysRevE.96.012411
[12] E.G. Iashina, S.V. Grigoriev, JETP, **129** (3), 455 (2019). DOI: 10.1134/S106377611908017X.